Cerebrovascular Impedance During Hemodynamic Change in Rabbits: A Pilot Study

Agnieszka Kazimierska, Magdalena Kasprowicz, Michał M. Placek, and Marek Czosnyka

Introduction

Cerebrovascular impedance describes the relationship between pulsatile arterial blood pressure (ABP) and pulsatile cerebral blood flow (CBF), i.e., the input and response of the cerebral vascular bed [1]. As a complex function of frequency, it is defined by modulus and phase shift, which represent respectively the amplitude ratio and phase difference between components of pressure and flow signals of corresponding frequency [2]. An impedance model of cerebral vascular bed that recognizes the frequency dependence of its parameters has been successfully used in studies on pulsatility index [3, 4] and critical closing pressure [5, 6]; however, while the link between vascular properties and impedance has been widely explored for most major vascular beds, relatively little is known about cerebrovascular impedance patterns [7, 8].

Traditionally, cerebrovascular impedance estimates are derived from Fourier spectra of CBF velocity (CBFV) and ABP [8], and the analysis is limited to steady-state conditions, fulfilling the signal stationarity requirements of Fourier transform. In this study, we propose an approach to calculate cerebrovascular impedance using heartbeat-to-heartbeat analysis and time-frequency methods, which allowed for the assessment of cerebrovascular impedance during controlled changes in ABP and intracranial pressure (ICP) in rabbits.

Materials and Methods

Material and Data Acquisition

A retrospective analysis of experiments conducted in New Zealand white rabbits between 1993 and 1997 was performed. The experiments were carried out in accordance with the standards established by the United Kingdom Animals (Scientific Procedures) Act of 1986. The experimental protocol is described in detail in [1, 9].

In short, the animals were anesthetized and supported in a sphinx position. The full group of 20 rabbits was divided into three subgroups, with each of the subgroups undergoing a different procedure: (a) in 8 rabbits a step decrease in ABP was induced by administration of trimetaphan, (b) in 5 rabbits a transient increase in ABP was induced by administration of dopamine, and (c) in 7 rabbits ICP was raised using constant-rate infusion (0.2 mL/min) of normal saline into the lumbar cerebrospinal fluid space.

ABP was recorded in the femoral artery with a direct pressure monitor inserted via a polyethylene cannula. CBFV was recorded in the basilar artery with an 8-MHz transcranial Doppler ultrasound probe positioned over a posterior frontal burr hole. In selected rabbits, ICP was recorded with a subarachnoid microsensor introduced through a second burr hole. The signals were collected using customized software at a sampling frequency ranging from 50 to 100 Hz.

A. Kazimierska (✉) · M. Kasprowicz
Department of Biomedical Engineering,
Faculty of Fundamental Problems of Technology, Wroclaw University of Science and Technology, Wroclaw, Poland
e-mail: agnieszka.kazimierska@pwr.edu.pl

M. M. Placek
Department of Biomedical Engineering,
Faculty of Fundamental Problems of Technology, Wroclaw University of Science and Technology, Wroclaw, Poland

Brain Physics Laboratory, Division of Neurosurgery,
Department of Clinical Neurosciences,
University of Cambridge, Cambridge, UK

M. Czosnyka
Brain Physics Laboratory, Division of Neurosurgery,
Department of Clinical Neurosciences,
University of Cambridge, Cambridge, UK

Institute of Electronic Systems, Faculty of Electronics and Information Technology, Warsaw University of Technology, Warsaw, Poland

B. Depreitere et al. (eds.), *Intracranial Pressure and Neuromonitoring XVII*, Acta Neurochirurgica Supplement 131,
https://doi.org/10.1007/978-3-030-59436-7_53,

Data Analysis

All analyses were performed using programs custom-written in MATLAB® (MathWorks®, Natick, MA, USA). Prior to analysis, all signals recorded at sampling frequencies under 100 Hz were upsampled to 100 Hz to ensure uniform sampling frequency across the whole data set. Phase-shift analysis was performed on signals bandpass filtered with cutoff frequencies of 1 and 20 Hz.

Selection of analysis period. First, signals were divided into individual heartbeats based on local minima of the CBFV signal. Duration of the analysis period extracted from each recording was expressed in heartbeats to account for variations in heart rate between the animals and during measurements. Due to the contrasting patterns of hemodynamic changes, different analysis periods were selected in each group: (a) for rabbits with arterial hypotension, 800 heartbeats before and 800 heartbeats after trimetaphan injection; (b) for rabbits with arterial hypertension, 100 heartbeats before and 1500 heartbeats after dopamine injection; and (c) for rabbits with intracranial hypertension, 200 heartbeats before and 2000 heartbeats after infusion onset. The time points corresponding to the administration of drugs or infusion onset were annotated manually. Extracted parts of the recording were subsequently used to obtain estimates of cerebrovascular impedance.

Modulus of cerebrovascular impedance. The modulus of cerebrovascular impedance ($|Z|$) describes the ratio of amplitudes of corresponding frequency components of ABP and CBFV [10]. At heart rate frequency, the modulus of cerebrovascular impedance (denoted $|Z(f_{HR})|$) is calculated as

$$\left|Z\left(f_{HR}\right)\right| = \frac{\mathrm{AMP}_{ABP}}{\mathrm{AMP}_{CBFV}} \tag{1}$$

where AMP_{ABP} and AMP_{CBFV} are the amplitudes of the fundamental harmonics of ABP and CBFV, respectively. In this work, to reduce the effect of changes in heart rate, amplitude estimates were calculated on a heartbeat-to-heartbeat basis as the difference between the systolic and the diastolic value of each signal.

Phase shift of cerebrovascular impedance. The phase shift of cerebrovascular impedance (PS) describes the time delay between corresponding frequency components of ABP and CBFV [2]. To follow PS in both time (i.e., during hemodynamic changes) and frequency (i.e., taking into account the changes in heart rate occurring during the experiment), a method of nonstationary signal processing called the joint time and frequency (TF) approach was used. In the TF approach, signals are represented on the two-dimensional time-frequency plane, which makes it possible to track their time-variant spectral content [11]. Here, the Zhao-Atlas-Marks (ZAM) distribution [12] was chosen to obtain estimates of TF phase shift (TFPS) between ABP and CBFV. This distribution is characterized by relatively high suppression of so-called interference cross-terms and limited trade-off between time and frequency resolution. The framework is described in detail in our previous work on the subject of cerebral autoregulation [13].

TFPS in the ZAM-distribution-based approach is calculated as [14]

$$\mathrm{TFPS}\left(t,f\right) = \arg\left[S_{\mathrm{ZAM},xy}\left(t,f\right)\right] \tag{2}$$

where $S_{\mathrm{ZAM},xy}(t, f)$ is the cross spectrum of signals x and y (here: ABP and CBFV). The cross spectrum (and, similarly, auto spectra of signals x and y, denoted by $S_{\mathrm{ZAM},xx}(t, f)$ and $S_{\mathrm{ZAM},yy}(t, f)$, respectively) is in turn described by the equation [15]

$$S_{\mathrm{ZAM},xy}\left(t,f\right) = \int_{-\infty}^{\infty} h\left(\tau\right)\mathrm{e}^{-j2\pi f\tau} \left[\int_{t-|\tau|/2}^{t+|\tau|/2} g\left(u-t\right)x\left(u+\frac{\tau}{2}\right)y*\left(u-\frac{\tau}{2}\right)du\right]d\tau \tag{3}$$

In the preceding equation, g and h are window functions responsible for smoothing the representation in time and frequency domain.

Here the TFPS representation obtained from Eq. (2) was further processed using a two-step masking procedure to extract areas that are both related to heart rate frequency and characterized by significant coupling between ABP and CBFV. To estimate the extent of coupling between the signals in the TF domain, magnitude-squared TF coherence (TFCoh) was used. TFCoh is described as [16]

$$\mathrm{TFCoh}\left(t,f\right) = \frac{\left|S^{(c)}_{\mathrm{ZAM},xy}\left(t,f\right)\right|^2}{S^{(c)}_{\mathrm{ZAM},xx}\left(t,f\right)\cdot S^{(c)}_{\mathrm{ZAM},yy}\left(t,f\right)} \tag{4}$$

where the superscript (c) indicates smoothing of the cross and auto spectra required to ensure that TFCoh is bounded to the range <0,1>. Only the (t, f) points of the TFPS representation where the corresponding TFCoh values exceeded the threshold value of 0.9 were included in further analysis [13]. Then a binary mask based on the fundamental frequency of ABP (i.e., the heart rate frequency) was applied to the coherence-filtered TFPS. A 3-decibel mask was obtained using the procedure proposed in [16] by first finding the maximum value in the TF representation of ABP around the heart rate frequency at each time instant and then locating the frequencies at which the value in the representation drops by 3 dB on either side of the maximum. Final time courses of PS at heart rate frequency ($\mathrm{PS}(f_{HR})$) were derived by averaging TFPS values along the frequency axis within the combined coherence- and ABP-based mask at each time instant. Time in seconds was then converted to dimensionless time expressed in heartbeats. Illustrative TF representations used to obtain $\mathrm{PS}(f_{HR})$ are presented in Fig. 1.

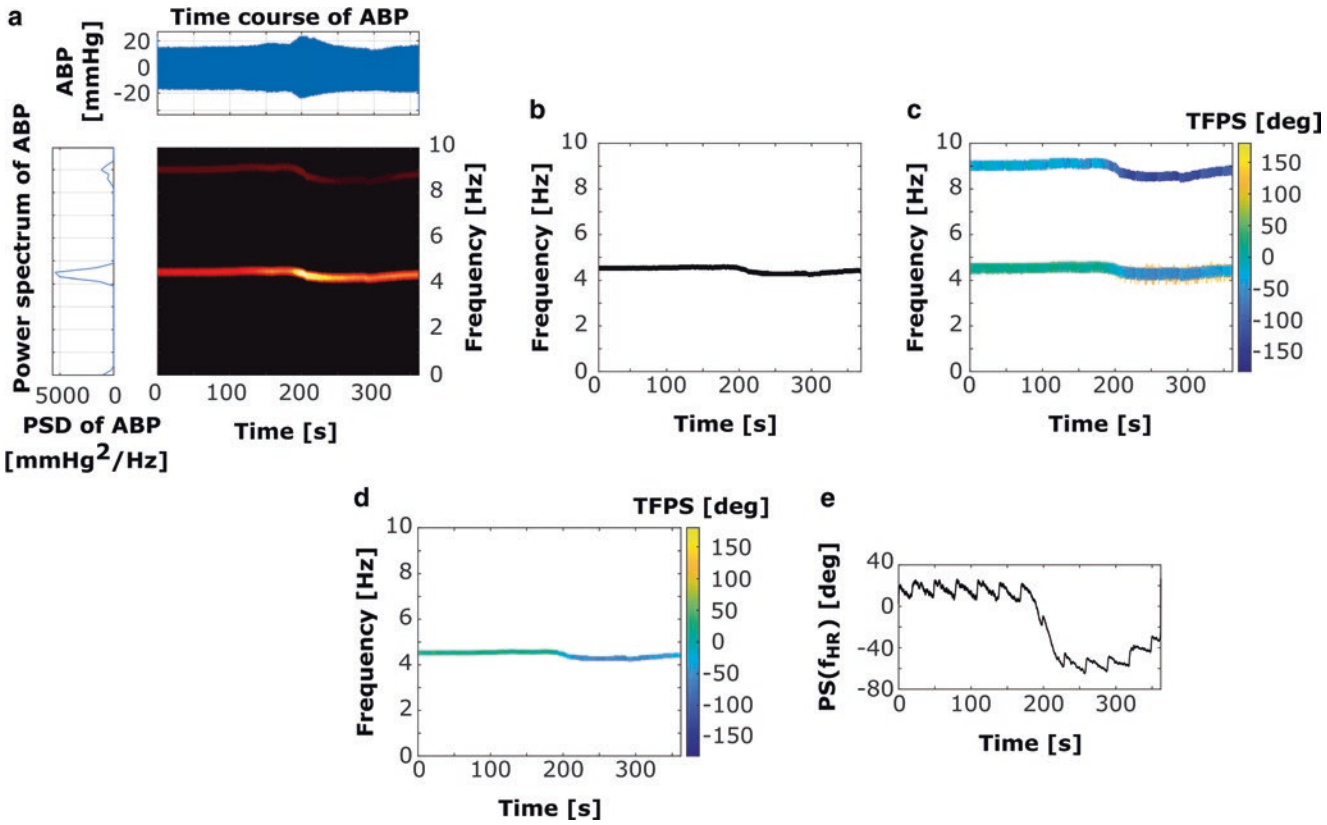

Fig. 1 Illustrative time-frequency representations used to obtain time course of phase shift of cerebrovascular impedance at heart rate frequency (PS(f_{HR})). (**a**) Bandpass-filtered time course (upper plot), power spectrum (left plot), and time-frequency auto spectrum (center graph) of arterial blood pressure (ABP). Note the fundamental harmonic of ABP around 4.5 Hz. (**b**) Binary mask based on the fundamental harmonic of ABP. Black areas indicate parts of the representation included in subsequent analyses. (**c**) Coherence-masked time-frequency phase shift (TFPS) between ABP and cerebral blood flow velocity (CBFV). White areas indicate parts of the representation where coherence between ABP and CBFV is lower than 0.9, which are excluded from subsequent analyses. (**d**) Coherence- and ABP-masked TFPS between ABP and CBFV obtained by overlaying mask presented in (**b**) on representation presented in (**c**). (**e**) Time course of PS(f_{HR}) values obtained from representation presented in (**d**)

Time courses of cerebrovascular impedance estimates. The time courses of $|Z(f_{HR})|$ and PS(f_{HR}) were compared with the time courses of mean ABP, ICP, and cerebral perfusion pressure (CPP; where available, estimated as CPP = ABP − ICP) calculated by averaging the signals over the period of one heartbeat. Illustrative time courses for one rabbit are presented in Fig. 2.

Results

Figure 3 shows the group-averaged time courses of impedance estimates and available parameters (ICP—and, consequently, CPP—was not recorded in the arterial hypertension group).

Following the injection of trimetaphan, mean ABP and mean CBFV both decreased (from the first 200 heartbeats to the last 200 heartbeats: ABP, decrease to 53% [52–57%] of baseline value; CBFV, decrease to 78% [52–96%]; values are presented as median [first-third quartile]). Similarly, CPP fell (to 45% [43–47%]) as mean ICP increased slightly (to 108% [93–172%]). $|Z(f_{HR})|$ decreased to 60% [45–74%] while PS(f_{HR}) changed from 25° [14°–66°] to –26° [−54° to 23°].

Conversely, following administration of dopamine, mean ABP increased (from the first 100 heartbeats to 100 heartbeats around the maximum of group-averaged mean ABP: an increase to 208% [119–214%]), as did mean CBFV (an increase to 117% [104–138%]). $|Z(f_{HR})|$ rose to 141% [123–168%] and PS(f_{HR}) changed from –34° [−50° to -27°] to –27° [−39° to –20°].

Saline infusion resulted in a mean ICP increase to 330% [315–370%] (from the first 200 heartbeats to the last 200 heartbeats), a mean CBFV decrease to 86% [80–98%], and a CPP decrease to 70% [67–82%]. No significant change was observed in either mean ABP or PS(f_{HR}), but $|Z(f_{HR})|$ dropped on average to 76% [69–109%].

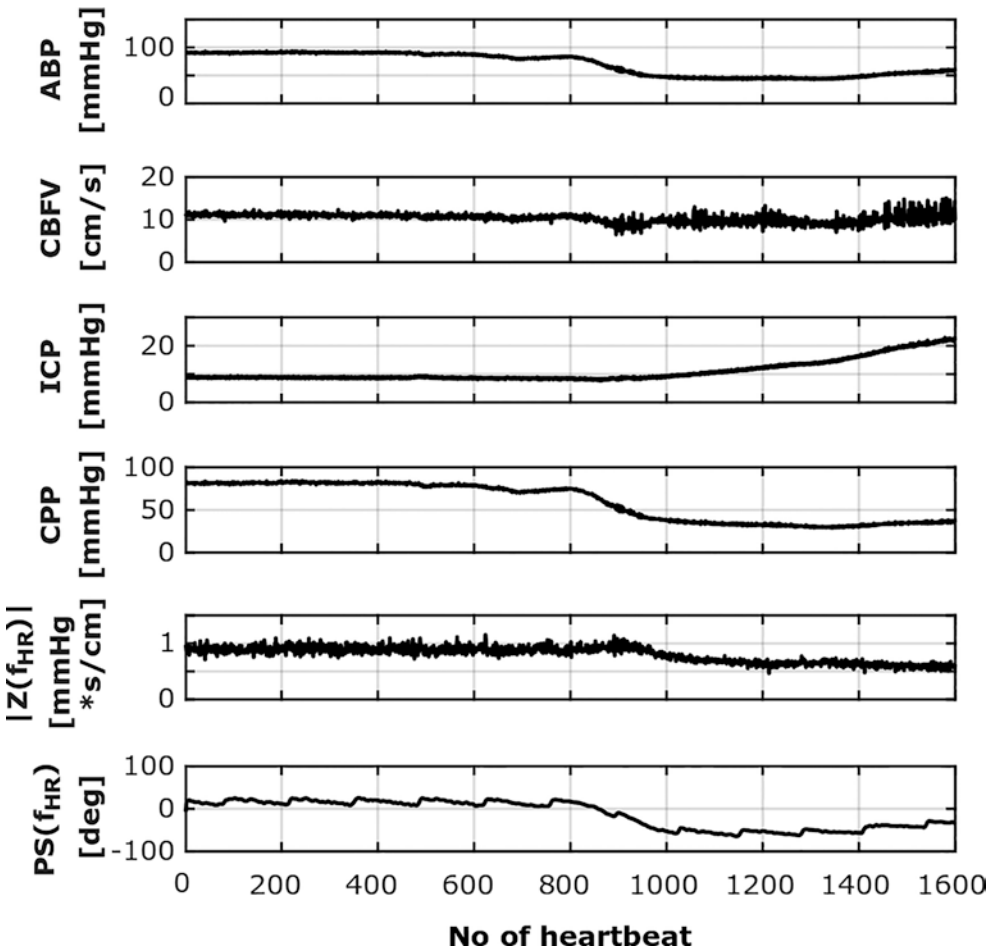

Fig. 2 Illustrative time courses for one rabbit from arterial hypotension group. Top to bottom: mean arterial blood pressure (ABP), mean cerebral blood flow velocity (CBFV), mean intracranial pressure (ICP), cerebral perfusion pressure (CPP), modulus of cerebrovascular impedance at heart rate frequency ($|Z(f_{HR})|$), and phase shift of cerebrovascular impedance at heart rate frequency ($PS(f_{HR})$)

Discussion

Frequency-dependent parameters describing cerebral hemodynamics are traditionally estimated using Fourier analysis [8]. However, the applicability of classical Fourier transform is restricted to steady-state conditions where the signals can be assumed to be stationary, significantly limiting the range of experiments where this approach is valid. On the other hand, the nonstationarity of biomedical signals, including those related to the cardiovascular system, has been widely recognized in recent years, leading to a rise in prominence of more advanced signal processing tools such as time-frequency methods [17]. The approach presented in this study was chosen specifically to offer the possibility of monitoring changes in cerebrovascular impedance estimates in time. In particular, the method of extracting heart-rate-related components of phase shift between ABP and CBFV, which takes into account the degree of coupling between them, uniquely supports tracking related changes despite the time-varying spectral content of the signals. Potential insights into phenomena governing cerebral hemodynamics offered by impedance analysis have been suggested by a number of studies that emphasized the importance of including frequency-dependent properties when interpreting indices describing the state of cerebral circulation in various conditions [3, 4, 8, 18]. In an attempt to extend cerebrovascular impedance analysis to transient hemodynamic changes, we have demonstrated that the proposed procedure allows for the assessment of modulus and phase shift of cerebrovascular impedance during controlled changes in systemic ABP and ICP.

Our results show that both $|Z(f_{HR})|$ and $PS(f_{HR})$ change during alterations in systemic ABP and follow the direction of changes in CPP, with increases observed in the hypertension and decreases in the hypotension group, while only $|Z(f_{HR})|$ is affected by changes in ICP. Interestingly, alterations in $PS(f_{HR})$ appear to depend not only on the magnitude but also the direction of change in ABP and its initial level, since we observed that baseline values of $PS(f_{HR})$ differ

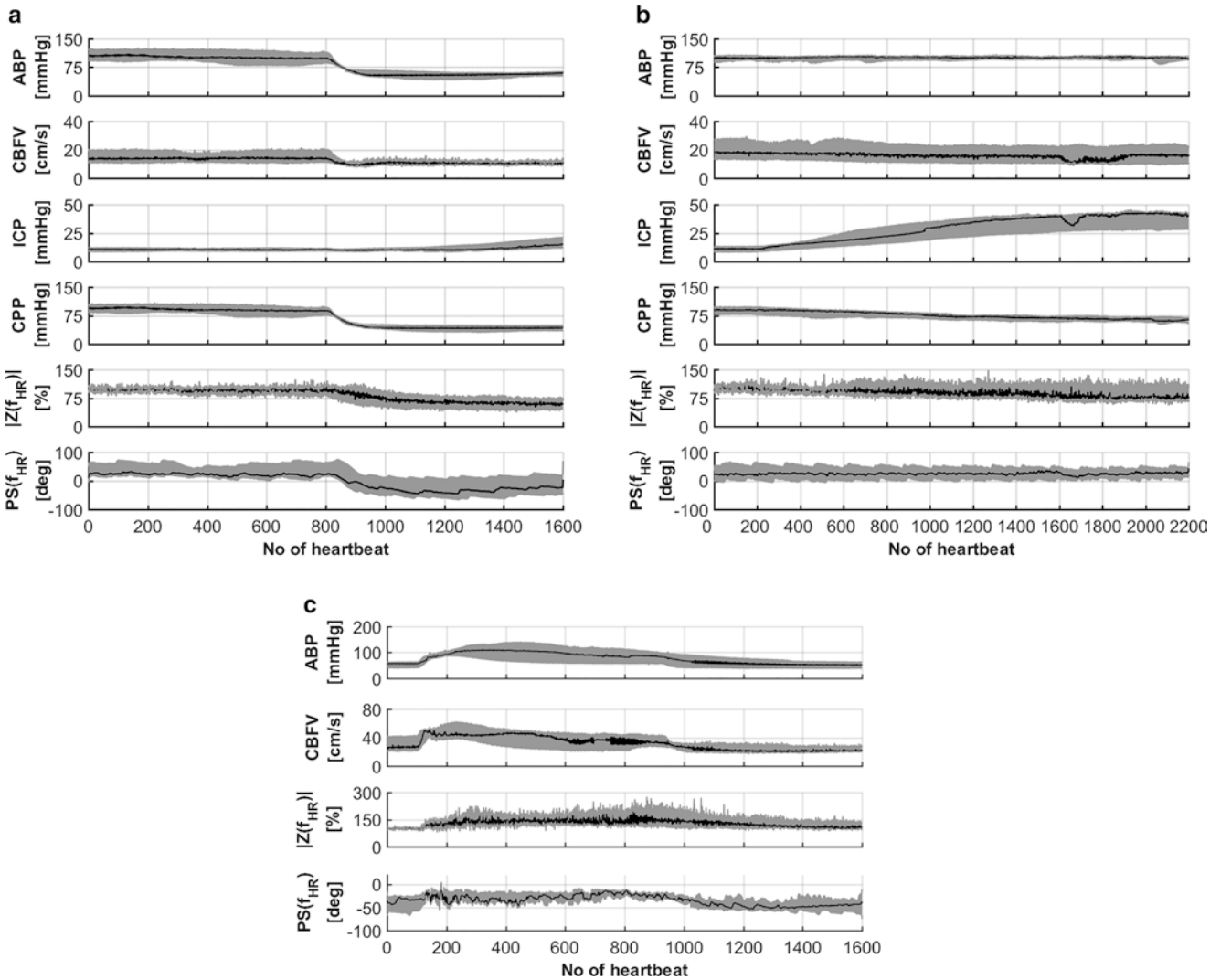

Fig. 3 Group-averaged time courses from (**a**) arterial hypotension, (**b**) intracranial hypertension, and (**c**) arterial hypertension group. Top to bottom: mean arterial blood pressure (ABP), mean cerebral blood flow velocity (CBFV), mean intracranial pressure (ICP; not included in part (**c**)), cerebral perfusion pressure (CPP; not included in part (**c**)), modulus of cerebrovascular impedance at heart rate frequency ($|Z(f_{HR})|$), and phase shift of cerebrovascular impedance at heart rate frequency ($PS(f_{HR})$). $|Z(f_{HR})|$ is presented as a percentage of baseline value. Black lines: median, gray area: interquartile range

between groups. The latter can be, at least in part, explained by the fact that the mean absolute ABP at baseline in the hypertension group (Fig. 3) corresponds to end rather than baseline level in the hypotension group. However, a comparable level of mean ABP reached after dopamine injection still did not produce positive $PS(f_{HR})$, which could be expected by comparison with the hypotension group. So far, phase relationships between ABP and CBFV have primarily been used to assess the state of cerebral autoregulation based on low-frequency components (i.e., below respiration frequency) [19], and little attention has been given to phase shift between signals related to cerebral pulsations in general. One previous study investigated the phase shift between the fundamental harmonics of CBFV and ICP during infusion tests and its relationship with diminished compensatory reserve at higher ICP levels [20]. This study, on the other hand, suggests an influence of the level of CPP on the characteristics of the cerebrovascular bed regarded as a system transferring pressure pulsations to pulsatile flow.

Limitations. In this study, transcranial Doppler measurements of CBFV in the basilar artery were used as estimates of pulsatile CBF, and ABP recordings in the femoral artery were used as substitutes for arterial pressure at brain level. It should be noted that CBFV is not a direct equivalent of the CBF waveform due to its dependence on the diameter of insonated vessels and the properties of the vascular bed, and femoral ABP is only an approximation of input cerebral pressure waveform (although it has been shown that in

humans the use of systemic ABP in modeling studies allows for fairly reliable estimation of CBF waveforms when used to replace cerebral pressure [21]). Moreover, the differences in pulse transit time between the heart and femoral and basilar arteries in individual recordings were not compensated, and the physical distance between measurement sites may have influenced the absolute values of PS(f_{HR}).

Acknowledgments M.C. is supported by NIHR Biomedical Research Centre, Cambridge, UK. The authors acknowledge support from the Polish National Agency for Academic Exchange under the International Academic Partnerships programme.

Conflicts of Interest **M.C. has a financial interest in the licensing fees of ICM+ software (https://icmplus.neurosurg.cam.ac.uk). The other authors declare that they have no conflict of interest.**

References

1. Czosnyka M, Richards H, Pickard JD, Harris N, Iyer V (1994) Frequency-dependent properties of cerebral blood transport—an experimental study in anaesthetized rabbits. Ultrasound Med Biol 20:391–399
2. O'Rourke MF (1982) Vascular impedance in studies of arterial and cardiac function. Physiol Rev 62:570–623
3. de Riva N, Budohoski KP, Smielewski P, Kasprowicz M, Zweifel C, Steiner LA, Reinhard M, Fabregas N, Pickard JD, Czosnyka M (2012) Transcranial Doppler pulsatility index: what it is and what it isn't. Neurocrit Care 17:58–66
4. Michel E, Zernikow B (1998) Gosling's Doppler pulsatility index revisited. Ultrasound Med Biol 24:597–599
5. Varsos GV, de Riva N, Smielewski P, Pickard JD, Brady KM, Reinhard M, Avolio A, Czosnyka M (2013) Critical closing pressure during intracranial pressure plateau waves. Neurocrit Care 18:341–348
6. Varsos GV, Richards HK, Kasprowicz M, Reinhard M, Smielewski P, Brady KM, Pickard JD, Czosnyka M (2014) Cessation of diastolic cerebral blood flow velocity: the role of critical closing pressure. Neurocrit Care 20:40–48
7. Tzeng YC, Chan GS (2011) Unraveling the human cerebral circulation: insights from cerebral blood pressure and flow recordings. J Appl Physiol (1985) 111:349–350
8. Zhu YS, Tseng BY, Shibata S, Levine BD, Zhang R (2011) Increases in cerebrovascular impedance in older adults. J Appl Physiol (1985) 111:376–381
9. Czosnyka M, Richards HK, Reinhard M, Steiner LA, Budohoski K, Smielewski P, Pickard JD, Kasprowicz M (2012) Cerebrovascular time constant: dependence on cerebral perfusion pressure and end-tidal carbon dioxide concentration. Neurol Res 34:17–24
10. Varsos GV, Kasprowicz M, Smielewski P, Czosnyka M (2014) Model-based indices describing cerebrovascular dynamics. Neurocrit Care 20:142–157
11. Wacker M, Witte H (2013) Time-frequency techniques in biomedical signal analysis. A tutorial review of similarities and differences. Methods Inf Med 52:279–296
12. Zhao Y, Atlas LE, Marks RJ (1990) The use of cone-shaped kernels for generalized time-frequency representations of nonstationary signals. IEEE Trans Acoust 38:1084–1091
13. Placek MM, Wachel P, Iskander DR, Smielewski P, Uryga A, Mielczarek A, Szczepanski TA, Kasprowicz M (2017) Applying time-frequency analysis to assess cerebral autoregulation during hypercapnia. PLoS One 12:e0181851
14. Orini M, Laguna P, Mainardi LT, Bailon R (2012) Assessment of the dynamic interactions between heart rate and arterial pressure by the cross time-frequency analysis. Physiol Meas 33: 315–331
15. Auger F, Flandrin P, Goncalves P, Lemoine O (1996) Time-frequency toolbox. http://tftb.nongnu.org/ Accessed 9 Nov 2020
16. Muma M, Iskander DR, Collins MJ (2010) The role of cardiopulmonary signals in the dynamics of the eye's wavefront aberrations. IEEE Trans Biomed Eng 57:373–383
17. Orini M, Laguna P, Mainardi LT, Bailon R (2017) Time-frequency analysis of cardiovascular signals and their dynamic interactions. In: Barbieri R, Scilingo EP, Valenza G (eds) Complexity and nonlinearity in cardiovascular signals. Springer, Cham, pp 257–287
18. Varsos GV, Richards H, Kasprowicz M, Budohoski KP, Brady KM, Reinhard M, Avolio A, Smielewski P, Pickard JD, Czosnyka M (2013) Critical closing pressure determined with a model of cerebrovascular impedance. J Cereb Blood Flow Metab 33:235–243
19. Diehl RR (2002) Cerebral autoregulation studies in clinical practice. Eur J Ultrasound 16:31–36
20. Kim DJ, Czosnyka M, Kim H, Baledent O, Smielewski P, Garnett MR, Czosnyka Z (2015) Phase-shift between arterial flow and ICP pulse during infusion test. Acta Neurochir 157: 633–638
21. Zamir M, Moir ME, Klassen SA, Balestrini CS, Shoemaker JK (2018) Cerebrovascular compliance within the rigid confines of the skull. Front Physiol 9:940